AIAA'83

AIAA-83-2094
Minimum-Fuel Aeroassisted Coplanar Orbit Transfer Using Lift Modulation

K.D. Mease, JPL/California Institute of Technology, Pasadena, CA; and N.X. Vinh, Univ. of Michigan, Ann Arbor, MI

AIAA Atmospheric Flight Mechanics Conference

August 15-17, 1983/Gatlinburg, Tennessee

A83-43812

MINIMUM-FUEL AEROASSISTED COPLANAR ORBIT TRANSFER USING LIFT-MODULATION*

K. D. Mease** and N. X. Vinh+

Abstract

Minimum-fuel trajectories and lift controls are computed for aeroassisted coplanar transfer from high orbit to low orbit. The optimal aeroassisted transfer requires less fuel than the all-propulsive Hohmann transfer for a wide range of high orbit to low orbit transfers. The optimal control program for the atmospheric portion of the transfer is to fly at maximum positive L/D initially to recover from the downward plunge, and then, to fly at negative L/D to level off the flight, such that the vehicle skips out of the atmosphere with a flight path angle near zero degrees. To avoid excessive heating rates, the vehicle flies initially at high angle of attack in order to slow down higher in the atmosphere, allowing recovery from the downward plunge, which occurs subsequently using the maximum positive L/D, to take place at a lower atmospheric density, or equivalently, at a higher altitude.

Nomenclature

b	R/H_e
B	$\rho_o S H_e C_L^*/(2m)$
C_D	drag coefficient
C_{D_o}	value of C_D when $C_L = 0$
C_L	lift coefficient
C_L^*	value of C_L at $(L/D)_{max}$
E^*	$(L/D)_{max}$
F	p_h/p_v
g	acceleration of gravity
GEO	Geostationary Earth Orbit
h	H/H_e
H	altitude
H_R	convective heating rate for 1m sphere
HEO	High Earth Orbit
K	coefficient in parabolic drag polar
L/D	lift-to-drag ratio
LEO	Low Earth Orbit
m	vehicle mass
OTV	Orbital Transfer Vehicle
p_i	adjoint variable associated with state i
r	radial distance from Earth's center
r_1	radius of HEO
r_2	radius of LEO
R	radius of spherical atmosphere
S	effective vehicle surface area normal to velocity vector
v	$V/\sqrt{\mu/R}$
V	inertial speed
α_i	r_i/R
γ	inertial flight path angle
δ	ρ/ρ_o
Δvi	$\Delta V_i/\sqrt{\mu/R}$
ΔV	impulsive change in V
ΔV_1	ΔV to deorbit from HEO
ΔV_2	ΔV to circularize at LEO
λ	C_L/C_L^*
Λ	$E^* p_\gamma/(v p_v)$
μ	gravitational constant multiplied by mass of Earth
ρ	atmospheric density
ρ_o	value of ρ at H = 40 km
τ	$(t/H_e)\sqrt{\mu/R}$

Subscripts

e	value at atmospheric entry
f	value at atmospheric exit
p	value at hypothetical perigee of transfer orbit from HEO to atmosphere

Introduction

When orbital transfer is required and there is an atmosphere-bearing celestial body in the vicinity, it may be advantageous to utilize aerodynamic force in effecting the transfer. In this paper, we present an investigation of aeroassisted coplanar transfer from a circular orbit of radius r_1 to a concentric circular orbit of radius r_2, where r_1 is greater than r_2 (Fig. 1). We will consider the orbits to be about the Earth, however much of the analysis is more generally applicable. Our assumptions are as follows. The vehicle has a lifting configuration; and the lift can be modulated by varying the angle of attack. Lift modulation is the sole means of controlling the flight path in the atmosphere, propulsion being used only outside the atmosphere. The vehicle has a high-thrust propulsion system so that applications of the thrust can be considered to produce impulsive velocity changes (ΔVs) and the fuel consumption for an orbital transfer is thus indicated by the characteristic velocity, the sum of the ΔVs needed to effect the transfer. The

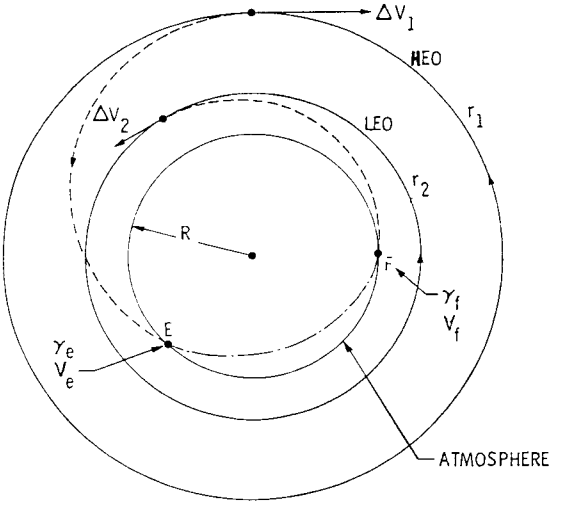

Fig. 1 Aeroassisted coplanar orbit transfer.

---

* The research described in this paper was carried out by the Jet Propulsion Laboratory, California Institute of Technology, under contract with the National Aeronautics and Space Administration.

** Member Technical Staff, Navigation Systems Section, Jet Propulsion Laboratory, California Institute of Technology, Pasadena, California, Member AIAA

\+ Professor, Aerospace Engineering, University of Michigan, Ann Arbor, Michigan

transfer must involve only a single atmospheric pass. And finally, the atmospheric properties, the vehicle's aerodynamic properties, the equations of motion, and the initial position and velocity of the vehicle are all known precisely.

Under these assumptions, we determine the minimum-fuel aeroassisted transfer, the fuel requirements of which are then compared to those of the minimum-fuel all-propulsive transfer. The characteristics of the minimum-fuel trajectory during the atmospheric portion of the aeroassisted transfer are examined in detail. In addition, the effect of a vehicle heating constraint on the atmospheric trajectory is determined.

The motivation for this study stems from the current interest in orbital transfer vehicles (OTVs).[1,2] These vehicles would transfer spacecraft from a space shuttle to higher and/or different inclination orbits. In the case of a space-based OTV, the vehicle is then required to return, after delivering its cargo, to rendezvous with either a shuttle or a space operations center. The OTV maneuvers which could potentially benefit from aeroassist are the orbital plane change and the transfer from high Earth orbit (HEO) to low Earth orbit (LEO). The present study concerns only the latter.

The basic sequence of events for the aeroassisted HEO to LEO coplanar orbit transfer is as follows. Referring to Fig. 1, the transfer begins with a tangential retroburn (ΔV_1) at HEO which injects the vehicle into an elliptical transfer orbit with a hypothetical target perigee inside the atmosphere. At point E, the vehicle enters the atmosphere. As the vehicle flies through the atmosphere, some of its kinetic energy is converted to heat, and consequently, upon skipping out of the atmosphere (at point F), the apogee of the orbit is decreased to the distance r_2. Finally, at the new apogee, a second tangential burn (ΔV_2) is executed to circularize and thereby achieve the desired LEO. The minimum-fuel aeroassisted transfer is that which has the minimum characteristic velocity, $\Delta V_1 + \Delta V_2$. The flight path for the minimum-fuel transfer is effected by the ΔV_1 magnitude, which controls the atmospheric entry, and the lift coefficient as a function of time during the atmospheric flight, which controls the exit and hence determines the required ΔV_2.

The above version of an aeroassisted transfer is somewhat restrictive. Firstly, a tangential ΔV_1 at HEO is not always the most fuel efficient means of effecting a transfer to specified atmospheric entry conditions. The justification for this restriction is that, for the range of HEO to LEO transfers considered in this paper, the additional fuel savings, if any, offered by non-tangential or multiple-impulse transfers, are small. Furthermore, multi-impulse transfers are often times impractical. For a more general treatment of the minimum-fuel deorbit, see Ref. 3. Secondly, the apogee of the transfer orbit, that the vehicle is in upon exiting the atmosphere, does not necessarily need to be at the distance r_2. However, for the one-impulse transfer from exit to LEO, this tangency turns out to be a property that is consistent with the minimum characteristic velocity transfer.

Analytic Solution for an Idealized Optimal Transfer

Consider an aeroassisted HEO to LEO transfer which proceeds as follows. Referring to Fig. 1, a tangential retroburn, ΔV_1, at HEO injects the vehicle into an elliptical transfer orbit with perigee at the distance R. When the vehicle is at perigee, its lifting capability (in this case, negative lift) is employed to effect flight along the boundary of the atmosphere (i.e., along a circular orbit of radius R). Flight along the boundary is continued until sufficient velocity has been depleted (by atmospheric drag) such that, upon reducing the lift to zero, the vehicle ascends on an elliptical orbit to an apogee at r_2. Finally, at r_2, a tangential circularizing burn, ΔV_2, is executed to achieve the desired LEO. The idealizations here are 1) that the atmospheric density at R is sufficient to generate enough drag to slow the vehicle in a reasonable amount of time and 2) that the vehicle has sufficient lift to maintain flight along the atmospheric boundary.

Now compare the characteristic velocity of this idealized transfer with that of any realistic aeroassisted transfer. A realistic transfer would require a larger ΔV_1 to ensure sufficient penetration into the atmosphere such that the required velocity is depleted before skipping back out, given the limited lifting capability of the vehicle. Thus the ΔV_1 for the idealized transfer is a lower bound for aeroassisted transfers. Secondly, for the one-impulse transfer from atmospheric exit to LEO, exit with a flight path angle of zero degrees ($\gamma_f = 0^o$) into an elliptical transfer orbit, tangent to LEO at apogee, leads to the minimum circularizing ΔV_2. The corresponding exit speed is $V_f = \sqrt{2\mu r_2/[R(r_2+R)]}$. Any other exit pair ($V_f$, γ_f) will lead to a higher ΔV_2. Consequently, the characteristic velocity, $\Delta V_1 + \Delta V_2$, for this idealized aeroassisted transfer is a lower bound for the characteristic velocity of any realistic aeroassisted transfer.

An analytic expression for this lower bound can be derived. Let

$$\alpha_1 = r_1/R \quad , \quad \alpha_2 = r_2/R \quad , \text{ and } \Delta v_i = \Delta V_i / \sqrt{\mu/R}$$

The elliptical grazing trajectory requires an impulse

$$\Delta v_1 = \sqrt{1/\alpha_1} - \sqrt{2/[\alpha_1(\alpha_1 + 1)]} \qquad (1)$$

The second impulse used to circularize the orbit at r_2 is

$$\Delta v_2 = \sqrt{1/\alpha_2} - \sqrt{2/[\alpha_2(\alpha_2 + 1)]} \qquad (2)$$

Thus the total characteristic velocity for the idealized aeroassisted transfer is

$$\Delta v_A = \Delta v_1 + \Delta v_2 \qquad (3)$$

Compare this to the characteristic velocity for the all-propulsive Hohmann transfer which is

$$\Delta v_H = \sqrt{1/a_1} - \sqrt{2a_2/[a_1(a_1+a_2)]} + \sqrt{2a_1/[a_2(a_1+a_2)]} - \sqrt{1/a_2} \quad (4)$$

The curve plotted in Fig. 2 represents pairs (a_1, a_2) for which $\Delta v_A = \Delta v_H$. For pairs below the curve, $\Delta v_A < \Delta v_H$, i.e., the idealized aeroassisted transfer requires less fuel. For example, idealized aeroassisted transfer from geostationary orbit to LEO requires less fuel than the Hohmann transfer, if the LEO radius, r_2 is less than about 12,000 km.

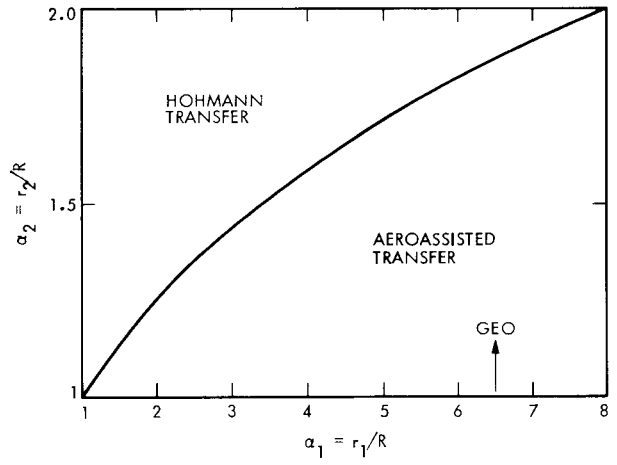

Fig. 2 Comparison of characteristic velocities for Hohmann and idealized aeroassisted transfers.

We now proceed to consider more realistic aeroassisted orbit transfer in which the vehicle flies a skip trajectory through the atmosphere. Determining the minimum-fuel trajectory and control, in this case, requires the formulation and numerical solution of an optimization problem.

Equations of Motion

The equations of motion for planar atmospheric flight are [4]

$$\frac{dr}{dt} = V \sin\gamma \quad (5a)$$

$$\frac{dV}{dt} = -\frac{\rho S C_D V^2}{2m} - g \sin\gamma \quad (5b)$$

$$V\frac{d\gamma}{dt} = \frac{\rho S C_L V^2}{2m} - \left(g - \frac{V^2}{r}\right)\cos\gamma \quad (5c)$$

assuming a nonrotating atmosphere. It is assumed that when $r > R$ the flight is Keplerian. Hence, we shall consider a Newtonian gravitational attraction, that is

$$g = \mu/r^2 \quad (6)$$

Furthermore, it is assumed that the drag polar is parabolic, that is

$$C_D = C_{D_o} + KC_L^2 \quad (7)$$

With this relation, using C_L as a control corresponds physically to using pitch modulation to shape the trajectory. It is convenient to use a normalized lift control

$$\lambda = C_L/C_L^* \quad (8)$$

where C_L^* is the lift coefficient corresponding to the maximum lift-to-drag ratio E^*. In terms of C_{D_o} and K, we have

$$C_L^* = \sqrt{C_{D_o}/K} \;;\; C_D^* = 2C_{D_o} \;;\; E^* = \frac{1}{2\sqrt{KC_{D_o}}} \quad (9)$$

Using the following dimensionless variables and parameters

$$h = H/H_e \;;\; v = V/\sqrt{\mu/R} \;;\; \tau = \frac{t}{H_e}\sqrt{\mu/R}$$

$$\delta = \rho/\rho_o \;;\; b = R/H_e \;;\; B = \frac{\rho_o S H_e C_L^*}{2m}$$

the equations of motion can be rewritten as

$$\frac{dh}{d\tau} = v \sin\gamma \quad (10a)$$

$$\frac{dv}{d\tau} = -\frac{B\delta}{2E^*}(1+\lambda^2)v^2 - \frac{b}{(b-1+h)^2}\sin\gamma \quad (10b)$$

$$\frac{d\gamma}{d\tau} = B\delta\lambda v + \frac{\cos\gamma}{(b-1+h)}\left[v - \frac{b}{(b-1+h)v}\right] \quad (10c)$$

Besides being preferable for numerical computation, the dimensionless equations of motion (10) focus attention on the critical aerodynamic parameters which affect flight, namely, the lift loading coefficient B and the maximum lift-to-drag ratio E^*. Again λ is the modulated lift control, scaled such that $\lambda = 1$ corresponds to flight at the maximum lift-to-drag ratio.

The Optimization Problem

The optimization problem is to find the magnitude of the tangential ΔV_1 and the lift control λ, as a function of time, which minimize the total characteristic velocity

$$\Delta v_1 + \Delta v_2 = \sqrt{1/a_1} - v_e\cos\gamma_e/a_1 + \sqrt{1/a_2} - v_f\cos\gamma_f/a_2 \quad (11)$$

Equivalently, we can maximize the function

$$L = v_e \cos\gamma_e/\alpha_1 + v_f \cos\gamma_f/\alpha_2 \qquad (12)$$

The atmospheric entry and exit variables must satisfy the relations

$$(2-v_e^2)\,\alpha_1^2 - 2\alpha_1 + v_e^2\cos^2\gamma_e = 0 \qquad (13)$$

and

$$(2-v_f^2)\alpha_2^2 - 2\alpha_2 + v_f^2\cos^2\gamma_f = 0 \qquad (14)$$

which are derived from the energy and angular momentum equations for the HEO-to-entry and exit-to-LEO transfer orbits, respectively. At entry we have

$$\tau_e = 0 \quad \text{and} \quad h_e = 1 \qquad (15)$$

and at exit

$$\tau_f = \text{free and } h_f = 1 \qquad (16)$$

We now proceed to derive necessary conditions for the optimal solution. Introducing adjoint variables p_h, p_v, and p_γ, we form the Hamiltonian

$$\mathcal{H} = p_h\, v\sin\gamma - p_v\left\{\frac{B\delta}{2E^*}v^2(1+\lambda^2) + \frac{b\sin\gamma}{(b-1+h)^2}\right\}$$

$$+ p_\gamma\left\{B\delta v\lambda + \frac{\cos\gamma}{(b-1+h)}\left[v - \frac{b}{(b-1+h)v}\right]\right\} \qquad (17)$$

With respect to the lift control λ, H is maximized when

$$\lambda = \frac{E^* p_\gamma}{v p_v} \qquad (18)$$

However, realistically the range of values which λ can assume is bounded, namely, the lift control must satisfy the inequality constraint

$$|\lambda| \le \lambda_{max} \qquad (19)$$

where λ_{max} is a positive constant whose value is dictated by the aerodynamic characteristics of the vehicle. According to the Maximum Principle, we find that the optimal lift control is determined by the rule

$$\lambda = \begin{cases} \lambda_{max} & \Lambda > \lambda_{max} \\ \Lambda & |\Lambda| < \lambda_{max} \\ -\lambda_{max} & \Lambda < -\lambda_{max} \end{cases} \qquad (20)$$

where $\Lambda = E^* p_\gamma/(v p_v)$. In determining this rule, we have used the fact that the Hamiltonian is a quadratic function of λ whose second derivative with respect to λ is negative.

The adjoint variables satisfy the necessary conditions

$$\frac{dp_h}{d\tau} = -\frac{\partial\mathcal{H}}{\partial h}\ ;\ \frac{dp_v}{d\tau} = -\frac{\partial\mathcal{H}}{\partial v}\ ;\ \frac{dp_\gamma}{d\tau} = -\frac{\partial\mathcal{H}}{\partial\gamma} \qquad (21)$$

However, note, that to compute the optimal control, only the value of Λ is required. This suggests replacing the three differential equations (21) with two which involve only ratios of the adjoint variables, namely Λ and $F = p_h/p_v$. Differentiating the expressions for Λ and F with respect to time and using Eqs.(21), we obtain

$$\frac{d\Lambda}{d\tau} = -E^*F\cos\gamma + \frac{\cos\gamma}{(b-1+h)^2 v}\left[\frac{2b\Lambda^2}{E^*} + bE^*\right]$$

$$+ \frac{\Lambda\sin\gamma}{(b-1+h)}\left[v + \frac{b}{(b-1+h)v}\right] \qquad (22)$$

and

$$\frac{dF}{d\tau} = -\frac{2b\sin\gamma}{(b-1+h)^3} + \frac{v\Lambda\cos\gamma}{E^*(b-1+h)^2}\left[v - \frac{2b}{(b-1+h)v}\right]$$

$$+ \frac{Bv^2}{2E^*}(1+\lambda^2)\delta' - \frac{v^2}{E^*}\Lambda B\lambda\delta' + F^2\sin\gamma$$

$$- \frac{FB}{E^*}\delta v(1+\lambda^2) + \frac{v}{E^*}\Lambda FB\delta\lambda$$

$$+ \frac{\Lambda F\cos\gamma}{E^*(b-1+h)}\left[v + \frac{b}{(b-1+h)v}\right] \qquad (23)$$

where

$$\delta' = \frac{d\delta}{dh} = \frac{H_e}{\rho_o}\frac{d\rho}{dH}$$

Writing the Hamiltonian in terms of Λ and F, we have

$$\mathcal{H} = F\sin\gamma - \frac{B}{2E^*}\delta v(1+\lambda^2) - \frac{b\sin\gamma}{(b-1+h)^2 v}$$

$$+ \frac{\Lambda B\delta v\lambda}{E^*} + \frac{\Lambda\cos\gamma}{E^*(b-1+h)}\left[v - \frac{b}{(b-1+h)v}\right] \qquad (24)$$

Since the equations of motion (10) do not depend explicitly on time and the final time is not prescribed, we have the Hamiltonian integral

$$\mathcal{H} = 0 \qquad (25)$$

Now, rather than the original six differential equations, we have five, namely, Eqs. (10) for the three states, and Eq. (22) and Eq. (23) for Λ and F. Integration of these equations will yield extremal trajectories for a number of problems which differ only in the entry and exit conditions which must be satisfied. Besides having reduced the dimension from six to five, this formulation has the distinct advantage that

four of the five dependent variables are physical variables. (Actually, Λ only has physical meaning if $|\Lambda| \leq \lambda_{max}$.) This situation eases the difficulty in guessing unknown initial conditions during the course of solving the boundary value problem. The nonphysical variable F can almost always ($\sin\gamma \neq 0$) be computed from the other four using the Hamiltonian integral (24). Indeed one might use the Hamiltonian integral to eliminate the need for solving the differential equation for F. However, to avoid the difficulty in evaluating F at the singularity, $\sin\gamma = 0$, we shall integrate the equation for F and instead use the Hamiltonian integral as a check on the accuracy of the numerical integration.

The heating rate, H_R, along the atmospheric trajectory is computed according to the equation

$$H_R = (3.08 \times 10^{-4})\ \rho^{1/2}\ V^{3.08} \qquad (26)$$

where ρ is the atmospheric density in kg/km^3 and V is the speed in km/s. Eq. 26 gives the convective heating rate for a sphere with a radius of one meter, under conditions of laminar flow. Since only relative changes are of concern, this model will suffice.

Method of Numerical Solution

We shall only concern ourselves with minimizing ΔV_2. Although ΔV_1 is the larger of the two burns, the difference between the value of ΔV_1, required to target to a perigee at the atmospheric boundary, R = 6498 km, and that, required to target to a perigee at the surface of the Earth, is a mere 13 m/s. In contrast, ΔV_2 is very sensitive to the values of the exit parameters v_f and γ_f. For example, the ΔV_2 required for a given HEO to LEO transfer can increase by 100 m/s or more for each degree above zero in the exit flight path angle, γ_f.

Knowing that a skip trajectory with $\gamma_f = 0^o$ leads to the minimum ΔV_2 at the LEO to which the ascending orbit is tangent, we employed the following approach to compute minimum-fuel trajectories and controls. A target perigee, r_p, is chosen and, from this, the entry parameters v_e and γ_e are determined according to the equations

$$v_e^2 = 2\left[1 - 1/(\alpha_1 + \alpha_p)\right] \qquad (27)$$

$$\cos^2\gamma_e = \left[2\alpha_1 - (2 - v_e^2)\ \alpha_1^2\right]/v_e^2 \qquad (28)$$

Then, using the computed values of v_e and γ_e, $h_e = 1$, and a pair (Λ_e, F_e) as initial conditions, Eqs. 10,22, and 23 are integrated from $\tau = 0$ to $h = 1$, using Eq. 20 to determine the lift control. The pair (Λ_e, F_e) is determined by choosing Λ_e and using Eq. 24 to solve for the corresponding value of F_e, with v, γ, and h as specified above. The integration is performed by a variable order, linear, multistep predictor-corrector routine of the Adams-Moulton type,[5] with the local absolute error controlled to less than 1.0×10^{-8} for each of the five dependent variables. In all cases studied, it has been possible to find, by iterative search, a value of Λ_e such that $\gamma_f = 0^o$ at exit. The corresponding value of v_f determines the apogee of the transfer orbit, following exit, and hence, the LEO to which the vehicle is optimally transferred. As the value of r_p is lowered from R, $\gamma_f = 0^o$ continues to be reachable, but the exit speed decreases, resulting in lower LEO transfers. There is a certain critical value of r_p, below which, the lifting capability of the vehicle is insufficient to effect a skip trajectory.

A trajectory and control computed in this manner is optimal in the following sense. Firstly, the necessary conditions (10), (22), and (23), the entry and exit conditions (15) and (16), and the relations (13) and (14) are satisfied. Secondly, the lift control satisfies the constraint (19). Thirdly, the near-zero degree flight path angle at exit ensures that the circularizing ΔV_2, to achieve the LEO to which the post-exit orbit is tangent, is the absolute minimum, when compared to those for all other aeroassisted transfers from the same HEO to the same LEO. (The exit flight path angles achieved, as indicated in Table 1, are a few tenths of a degree. The iteration on Λ_e was stopped at this point because the associated value of ΔV_2 was within 8 m/s of the lower bound set by the idealized transfer.) Fourthly, although only ΔV_2 has been minimized, the characteristic velocity, $\Delta V_1 + \Delta V_2$, is very close to the absolute minimum. The value of ΔV_1 for the cases shown in Table 1 is within 10.4 m/s of the lower bound on ΔV_1 given by the idealized transfer. Thus, the characteristic velocity can not get much smaller. More important, however, is whether the trajectory and/or control would change significantly, as the characteristic velocity is reduced the last few meters per second. Numerical experience indicates that they do not. As the exit flight path angle is reduced, the atmospheric trajectory is changing very little. Indeed, the value of Λ_e is being changed only slightly (parts in 10^6 or less) to get the exit angle below a few tenths of a degree. This level of change in Λ_e affects most of the trajectory almost negligibly, but extends the trajectory, in order to achieve the lower exit angle. Furthermore, as mentioned above, for zero exit flight path angle atmospheric trajectories, there is a one-to-one mapping, based on numerical experience, from values of r_p to values of v_f, and hence, to the LEOs for which the ΔV_2 is a minimum. Therefore, if r_p were increased in order to decrease ΔV_1, the corresponding ΔV_2 would be greater. Given the low sensitivity of ΔV_1 to changes in the value of r_p, it is unlikely that the characteristic velocity could be reduced much, if any, by adjusting r_p. In conclusion, a trajectory and control, computed in the manner described above, is a good approximation to that with the absolute minimum characteristic velocity and, henceforth, we shall refer to such a solution as a minimum-fuel solution.

When a heat rate constraint is imposed, the solution procedure is somewhat different. We follow an approach used in Ref. 6. The heating rate for a skip trajectory reaches its maximum value shortly after entry, in a monotonic fashion (see Fig. 4). It then decreases during the remainder of the flight, although some oscillation may occur. In order to satisfy a heating rate constraint, $H_R \leq (H_R)_{max}$, we shall assume that it

is sufficient to control the first peak of the heating rate function, such that the peak value is equal to $(H_R)_{max}$. Furthermore, we shall assume that, once this peak value is reached, flight does not continue on the constraint boundary. These assumptions allow us to solve the constrained problem in two stages each requiring an iteration on only one parameter.

In the first stage, we begin at τ=0 as in the unconstrained case, except that now the goal is to choose Λ_e such that $H_R = (H_R)_{max}$ at the time when the derivative of the heating rate with respect to time is equal to zero. Once this value of Λ_e is found, an extremal trajectory up to the peak heating rate is determined. The second stage is to find a value for Λ, $\Lambda = \Lambda_p$, such that, when Eqs. 10, 22, and 23 are integrated from the time of the peak heating rate to atmospheric exit, the exit flight path angle is zero degrees. Indeed, in the cases studied, it has been possible to find such values of Λ_e and Λ_p. Thus, the functions Λ and F are, in general, discontinuous at the time of the peak heating rate; the states h, v, and γ are always continuous.

Minimum -Fuel Trajectories

For all the cases reported below, the transfer is from geostationary Earth orbit (GEO), for which r_1 = 42,241 km. The radius of the atmosphere is 6498 km. Above this distance, the density is identically zero. Over the altitudes of atmospheric flight, 40-120 km (where the radius of the Earth is taken to be 6378 km), the density is approximated by a fifth-degree Chebyshev polynomial whose coefficients were determined by a least-squares fit to the U.S. Standard Atmosphere, 1976 (Ref. 7). The vehicle mass-to-surface area is 300 kg/m^2 for all cases.

Unconstrained

We begin by presenting some minimum-fuel trajectories, under conditions of unbounded lift ($\lambda_{max} \to \infty$) and unconstrained heating rate. Three vehicle configurations were considered, as distinguished by their respective maximum L/D capabilities, namely, 0.845, 1.5, and 2.9. Data from wind tunnel tests is available for vehicles with these maximum L/D capabilities (Refs. 8,9, and 10, respectively) and the values for the parameters C_{D_o} and K which appear in the parabolic drag polar were chosen to best fit the data. The values used for the pair (C_{D_o}, K) were (0.21, 1.67), (0.10, 1.11), and (0.017, 1.76), respectively.

For each of the three maximum L/D cases, we have fixed r_p = 6400 km and have searched and found the Λ_e such that $\gamma_f = 0^o$. In this manner, a minimum-fuel trajectory for each case was generated. The corresponding LEO orbits, to which the transfers are optimal, are not exactly the same, but are close enough to permit comparisons. The alternative approach of specifying the LEO orbit a priori would require searching on two parameters, r_p and Λ_e, in order to determine the minimum-fuel trajectory.

Certain characteristics of the minimum-fuel unconstrained trajectories are given in the first three columns of Table 1. We see that the high L/D vehicle penetrates farthest into the atmosphere and experiences the highest dynamic pressure and heating rate. The low L/D vehicle experiences the highest g-load. For comparison, the Shuttle design limits for dynamic pressure and g-load are 16 kN/m^2 and 2.5 respectively.[11] Time histories of the state variables for the $(L/D)_{max}$ = 1.5 case are shown in Fig. 3; those for the heating rate,

Table 1. Characteristics of minimum-fuel trajectories

	L/D Capability			Heating Rate	
	Low	Moderate	High	Unconstrained	Constrained
$(L/D)_{max}$	0.845	1.5	2.9	1.5	1.5
Target perigee r_p (km)	6400.0	6400.0	6400.0	6415.0	6415.0
Λ_e (Λ_p)	2.303247	2.701724	3.2586836	2.947660826	6.56(.79867315)
Exit flight path angle (deg)	0.3	0.4	0.3	0.45	0.49
LEO orbit radius (km)	6558.8	6578.7	6557.6	6608.0	6625.0
ΔV_2 (m/s)	26.1	31.0	25.2	40.5	45.1
Ideal ΔV_2 for same LEO (m/s)	18.3	24.0	18.0	32.6	37.7
Min altitude (km)	58.8	58.2	51.5	61.2	64.0
Max dynamic pressure (kN/m^2)	15.9	18.6	44.2	13.1	8.8
Max convective heating rate for a one meter sphere (W/cm^2)	193.1	222.8	361.4	190.8	150.0
Max g's	3.6	2.7	1.8	1.9	3.7

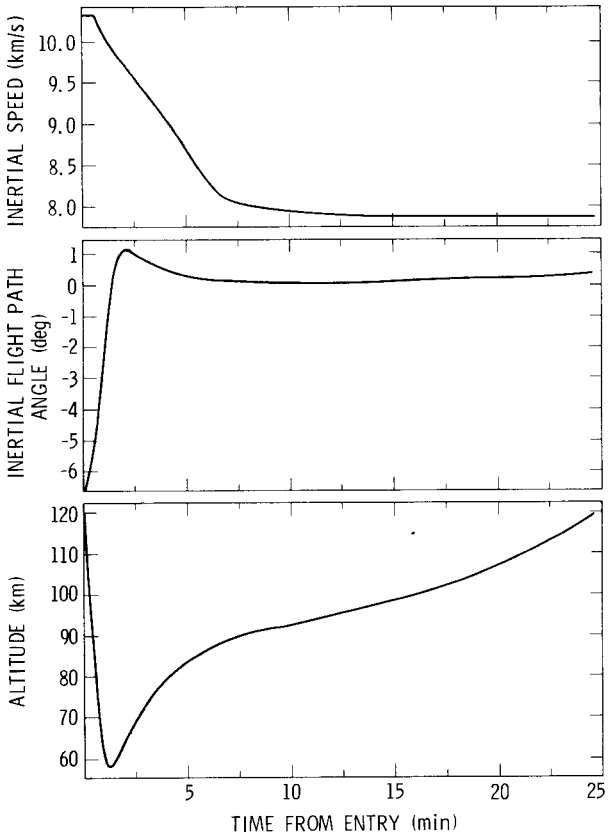

Fig. 3 Time histories of state variables, $(L/D)_{max} = 1.5$.

dynamic pressure, and g-load are shown in Fig. 4. The behaviors illustrated in these two figures are qualitatively representative of all the cases investigated in this paper.

Fig. 5 shows the lift-to-drag ratio as a function of the time from atmospheric entry for the three cases. A similar pattern is followed in each case. The maximum positive L/D is used initially to recover from the downward plunge. As the flight path angle becomes positive, the maximum negative L/D is used to level off the flight. These first two phases occur within the first four minutes of flight. Of course, although the basic pattern is similar, quantitatively, there are definite differences in the flight characteristics of the three L/D vehicles, as indicated in Table 1. After the first four minutes, a negative L/D is used to maintain flight at a small positive flight path angle in order to achieve the desired shallow exit. The required negative L/D increases, as the flight proceeds, to compensate for the decreasing atmospheric density.

Bounded Lift

For the vehicle, with $(L/D)_{max} = 1.5$, wind tunnel data show that the lift coefficient does not exceed 0.9 in absolute value. Thus, we impose the constraint

$$|C_L| \leq 0.9$$

which corresponds to setting $\lambda_{max} = 3.0$ in Eq. 20. The resulting lift control is given by the dashed curve in Fig. 6. For comparison, the

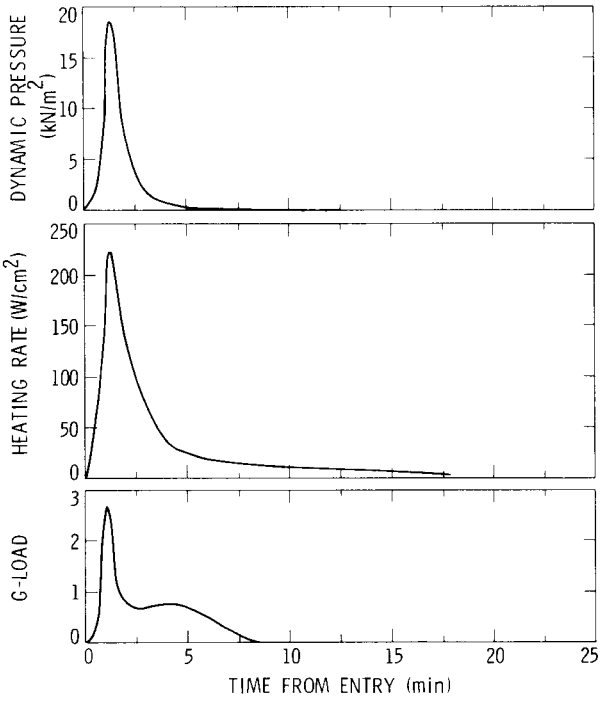

Fig. 4 Time histories of heating rate, dynamic pressure, and g-load, $(L/D)_{max} = 1.5$.

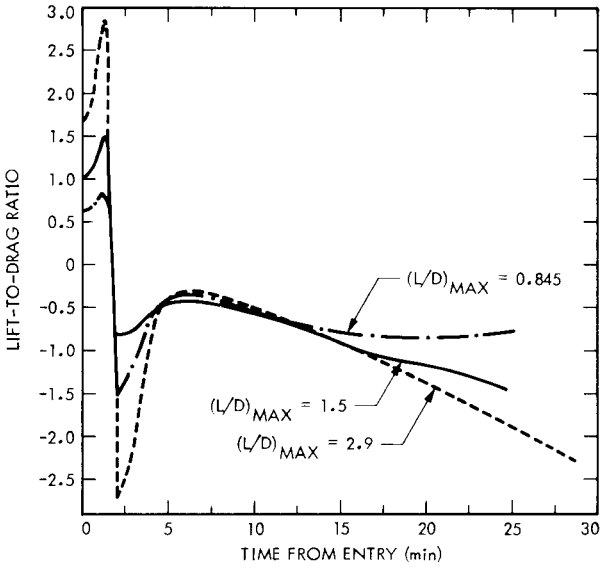

Fig. 5 Time histories of lift-to-drag ratio.

corresponding curve with C_L unbounded is given by the solid curve. We see that flight is along the constraint boundary for much of the flight. The important point, however, is that a near zero exit flight path angle is still reachable by proper choice of Λ_e.

Constrained Heating Rate

Using Eq. 26, the heating rate along the minimum-fuel trajectory can be calculated. Referring to this as the unconstrained heating rate, we can ask the question: What is the minimum-fuel trajectory, if the maximum heating

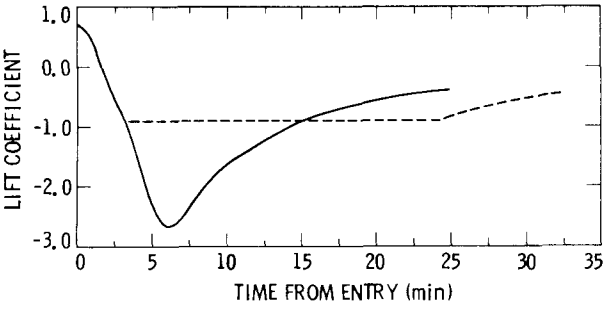

Fig. 6 Time histories of optimal lift control for unbounded and bounded cases.

rate is constrained to be no greater than some fraction of the maximum unconstrained heat rate?

In order to see the effect of a heating rate constraint, we again consider the configuration with $(L/D)_{max} = 1.5$, as described earlier, except that the target perigee is taken to be 6415 km. The minimum-fuel trajectory is computed first with the heating rate unconstrained. The maximum heating rate is found to be 190.8 W/cm^2 for a reference one meter sphere. Next, the minimum-fuel trajectory is computed with all conditions identical, except that the heating rate is constrained not to exceed 150.0 W/cm^2. In both cases, the lift coefficient is bounded, as described earlier.

Certain characteristics of the unconstrained and constrained cases are given for comparison in the last two columns of Table 1. In both cases, a near-zero exit flight path angle is reachable and the ΔV_2 is within 8 m/s of that for the idealized transfer. With the heating rate constrained, the vehicle does not penetrate the atmosphere as deeply, the maximum dynamic pressure is reduced, but the maximum g-load is increased.

The optimal lift control, for each case, is plotted versus time in Fig.7 . We see that the vehicle flies, initially, at $(C_L)_{max}$, in the constrained case; whereas, in the unconstrained case, C_L is decreasing steadily during the same period. By flying at $(C_L)_{max}$ initially, and correspondingly at a higher C_D, the vehicle slows down higher in the atmosphere, allowing recovery from the downward plunge, which occurs subsequently at the maximum positive L/D, to take place at a lower atmospheric density or equivalently at a higher altitude. In this manner, higher heating rates are avoided.

As a final note, the minimum entry flight path angle from which the vehicle can recover and achieve the prescribed exit state conditions, is raised when a heating rate constraint is imposed (that is, raised with respect to the unconstrained case). The reason is that, if the entry is too steep, even by flying at the maximum positive C_L, excessive heating rates cannot be avoided. In the particular case investigated here, an optimal solution was found for entry angles as low as -6.5^o (r_p = 6400 km) in the unconstrained case. In the constrained case, the lowest entry angle, that could be tolerated, was -6.0^o (r_p = 6415 km).

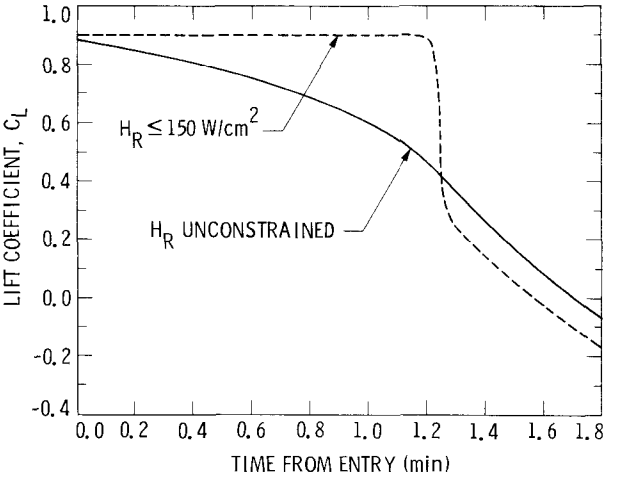

Fig. 7 Time histories of optimal lift control for unconstrained and constrained heating rate cases. (Only first two minutes shown.)

Summary and Conclusions

Under the assumptions and restrictions given in the Introduction, minimum-fuel aeroassisted coplanar transfer from high orbit to low orbit has been considered. An idealized version of the transfer lent itself to analytic treatment and allowed a lower bound on the characteristic velocity for any given HEO to LEO aeroassisted transfer to be determined. In order to examine minimum-fuel transfer under more realistic conditions, an optimization problem was formulated and solved numerically. It was found that for each given HEO to LEO transfer considered, even with bounded lift and/or a heating rate constraint, a characteristic velocity within 10-20 m/s of the lower bound is achievable. Thus, Fig. 2 provides a good indication of the high orbit to low orbit coplanar transfers for which the optimal aeroassisted transfer requires less fuel than the Hohmann transfer.

The characteristic lift program for the atmospheric portion of the minimum-fuel transfer is to fly at the maximum positive L/D initially to recover from the downward plunge, and then, to fly at negative L/D to level off the flight, such that the vehicle skips out of the atmosphere with a flight path angle near zero degrees. This program is modified at the beginning if high heating rates are to be avoided. Flight initially at maximum lift, and correspondingly, high drag, lowers the vehicle's speed higher in the atmosphere, allowing recovery from the downward plunge, which occurs subsequently using the maximum positive L/D, to take place at a lower atmospheric density, or equivalently, at a higher altitude.

References

1. Cruz, M. I., French, J. R., and Austin, R. E., 'System Design Concepts and Requirements for Aeroassisted Orbital Transfer Vehicles,' Paper No. 82-1379, AIAA 9th Atmospheric Flight Mechanics Conference, San Diego, CA, Aug. 1982.

2. Walberg, G.D., 'A Review of Aeroassisted Orbit Transfer,' Paper No. 82-1378, AIAA 9th Atmospheric Flight Mechanics Conference, San Diego, CA, Aug. 1982.

3. Buseman, A. and Vinh, N.X., 'Optimum Constrained Disorbit by Multiple Impulses,' Journal of Optimization Theory and Applications, Vol. 2, No. 1, 1968, pp. 40-64.

4. Vinh, N.X., Optimal Trajectories in Atmospheric Flight, Elsevier Scientific Publishing Company, New York, 1981.

5. Krogh, F. T., 'VODQ/SVDQ/DVDQ - Variable Order Integrators for the Numerical Solution of Ordinary Differential Equations,' JPL Technical Utilization Document No. CP-2308, NPO-11643, May 1969.

6. Chern, J. S., Yang, C. S., Vinh, N. X., and Hwang, G. R., 'Optimal Three-Dimensional Reentry Trajectories Subject to Deceleration and Heating Constraints,' Paper No. 82-309, 33rd Congress of the International Astronautical Federation, Paris, France, Sept. 1982.

7. 'U.S. Standard Atmosphere, 1976,' NOAA-S/T 76-1562, U.S. Government Printing, Washington, D.C.

8. Penland, J.A., 'A Study of the Stability and Location of the Center of Pressure on Sharp, Right Circular Cones at Hypersonic Speeds,' NASA TN D-2283, 1964.

9. Miller, C. G. and Gnoffo, P. A., 'An Experimental Investigation of Hypersonic Flow Over Biconics at Incidence and Comparison to Prediction,' Paper 82-1382, AIAA Atmospheric Flight Mechanics Conference, San Diego, CA, Aug. 1982.

10. Brooks, C.W., Jr. and Cone, D., Jr., 'Hypersonic Aerodynamic Characteristics of Aircraft Configurations with Canard Controls,'NASA TN D-3374, 1966.

11. Harpold, J.C. and Graves, C. A., Jr., 'Shuttle Entry Guidance,' Journal of the Astronautical Sciences, Vol. 27, No. 3, July 1979, pp. 239-268.